Construction and Building Materials 453 (2024) 139090

Contents lists available at ScienceDirect

Construction and Building Materials

journal homepage: www.elsevier.com/locate/conbuildmat

Mechanical, rheological and functional consequences of healing of porous asphalt mixtures by magnetic induction

Christopher DeLaFuente-Navarro [a,b], Pedro Lastra-González [a], Irune Indacoechea-Vega [a], Daniel Castro-Fresno [a,*]

[a] GITECO Research Group, Universidad de Cantabria, Avda. de Los Castros s/n, Santander 39005, Spain
[b] School of Civil Construction, Faculty of Engineering, Pontificia Universidad Católica de Chile, Avenida Vicuña Mackenna, Santiago 4860, Chile

ARTICLE INFO

Keywords:
Porous asphalt mixture
Self-healing
Magnetic induction consequences
Magnetic by-product

ABSTRACT

Magnetic induction technology has been extensively developed so far. However, the mechanical, rheological and functional consequences of repeated self-healing are still unknown. For this reason, this paper investigates the consequences of repeated healing cycles by magnetic induction in four chapters: first, the healing temperature of the experimental mixtures was determined and compared with a reference mixture, that was left to stand at room temperature for 90 days to assess the actual self-healing capacity of the asphalt mixtures. Second, the performance against particle loss was evaluated by applying different healing cycles in the cantabro test and particle loss by brush test. Third, rheological consequences on the binder were determined by penetration, ring and ball and dynamic shear rheometer. Fourth, functional consequences on the mixture were studied in terms of permeability and noise absorption capacity. In this way, we are analyzing the impact of the healing cycles on the mechanical performance of the mixture, the properties of the binder and the functional properties respectively. Regarding the results, healing by magnetic induction in porous asphalt mixtures reduces particle loss to a third. Furthermore, there are no statistically significant differences in the performance of the residual binders of the reference mixture without healing cycles and the residual binder of the experimental mixtures after 20 healing cycles. Finally, with respect to their functional properties, repeating the healing cycles 20 times produces a small decrease in the permeability capacity, which is not statistically significant. At the same time, repeated healing cycles significantly increase the noise absorption capacity of the asphalt mixture, possibly due to a slight draining of the binder, which increases the porosity at the top of the mixtures.

1. Introduction

Asphalt mixtures can be self-healing. This property depends on the temperature and the rest time of the asphalt [1]. Unfortunately, the self-healing process of asphalt materials at room temperature is very slow and needs a long rest period [2–4]. For this reason, various authors have developed methods to accelerate the self-healing process. In this respect, magnetic induction technology has shown considerable potential for accelerating the self-healing of cracks in the pavement [3,5,6].

The magnetic induction healing method is based on the addition of a magnetic aggregate to the asphalt mixture at the manufacturing phase [7]. This allows the pavement to receive preventive maintenance by applying a magnetic field to heal micro-cracks, preventing the formation of macro-cracks. This is possible because the magnetic field induces a current through the pavement, which due to the electrical resistance of the materials increases the temperature of the mixture, decreasing the viscosity and dilating the asphalt binder. Cracks are healed by molecular diffusion due to the thermal effect of the conductive materials [8–10].

This technology has been extensively studied and it is now possible to design inductive asphalt mixtures with magnetic induction healing capability [11–14]. To date, it has been found that there is an optimal healing temperature, as overheating can cause swelling of the specimens, which will decrease healing [15,16]. In this respect, it is important to note that healing does not only occur during the induction heating time, but also during the cooling time [17]. In addition, magnetic induction technology can heal cracks up to a width of 0.639 mm [18], after which healing efficiency decreases [19]. Also, the healing by magnetic induction can be repeated [20–22]. However, the efficiency of

* Corresponding author.
E-mail addresses: Christopher.delafuente@unican.es (C. DeLaFuente-Navarro), Pedro.lastragonzalez@unican.es (P. Lastra-González), Irune.indacoechea@unican.es (I. Indacoechea-Vega), Castrod@unican.es (D. Castro-Fresno).

https://doi.org/10.1016/j.conbuildmat.2024.139090
Received 12 July 2024; Received in revised form 24 October 2024; Accepted 5 November 2024
Available online 7 November 2024

the healing decreases with each healing cycle [7,23]. The reasons for this are controversial among researchers, with some authors maintaining that bitumen does not age through induction heating because it is a very short thermal process [24], and other authors claiming that healing by magnetic induction does produce an ageing of the binder [25]. This is an important point because the self-healing capacity depends on the type of binder and its degree of ageing [26,27]. In addition, it has been found that the composition and size of the magnetic particles directly affect the heating process [28]. That is, bigger and longer particles are more useful because they improve the heating rate [29,30]. Furthermore, the speed of heating is influenced by the number of magnetic particles contained in the mixture [31]. In this respect, there is an optimal content of magnetic particles [32], beyond which clusters begin to form, leading to uneven heating of the pavements [33,34].

To date, despite many advances in this technology, researchers have not investigated the impact and consequences of repeated healing cycles on porous asphalt mixtures. This is very important because porous asphalt mixtures are used for increasing roads safety [35,36], as they increase the skid resistance [37], improve stormwater run-off [38,39] and control noise contamination [40–43]. Unfortunately, the impact of healing by magnetic induction on durability in terms of particle loss is still unknown. Furthermore, although it has been mechanically proven that the healing process can be repeated [22,23], the consequences of repeated healing cycles are unclear: the potential degradation of the asphalt binder is undefined, and the functional consequences of repeated healing cycles are unknown.

For these reasons, the objective of this research was to determine the impact of different healing cycles on the particle loss performance of porous asphalt mixtures. In addition, the healing cycles were repeated 20 times and the rheological consequences on the binder and the functional consequences on permeability and sound absorption were determined. Achieving the objective of this study will clarify the feasibility of repeating the healing cycles by magnetic induction. If its feasibility is verified, it would be a viable option to solve the ravelling characteristic of this type of mixtures, without significantly compromising their functional properties.

To meet the objective of this research, three hot porous asphalt mixtures were designed: a reference mixture without magnetic aggregate and two experimental mixtures, one with virgin steel fibers (Exp. 1) and the other one with industrial by-product as magnetic aggregate (Exp. 2).

The investigation was divided into four phases: firstly, the optimum healing temperature was determined by means of a rupture-healing-rupture test; secondly, the mixtures were subjected to the cantabro test and the surface particle loss test by applying different healing cycles; thirdly, the rheological consequences of repeated healing cycles on the mixture compared to the binder of the three mixtures were determined by ring and ball test, penetration, dynamic shear rheometer; and finally, the consequences of repeated healing cycles on the permeability and noise absorption were evaluated.

2. Materials, samples fabrication and research methodology

2.1. Materials

Polymer modified asphalt binder type PMB 45/80–65, typically used in porous asphalt mixtures, was used [13,44]. Properties are summarized in Table 1. In addition, the natural aggregates were ophite for the coarse fraction and limestone for the fine and filler fractions, whose properties are shown in Table 2.

Two types of magnetic aggregates were used: virgin steel fibers (density: 7.850 g/cm^3) and steel shot (density: 7.435 g/cm^3) which is an industrial by-product (Fig. 1).

Table 1
Properties of binder.

Binder type	Test	Value	Standard
PMB	Penetration (25°C, mm/10)	61	EN 1426
	Specific Gravity	1.029	EN 15326
	Softening point (°C)	72.9	EN 1427
	Cohesion (5°C, J/cm^2)	7.14	EN 13703
	Elastic recovery (25°C, %)	90	EN 13398

2.2. Samples fabrication

For the development of this research, three asphalt mixtures were designed, as summarized in Table 3. All the asphalt mixtures studied had the same particle size distribution (Fig. 2). The use of the industrial by-product is intended to assess the possibility of replacing virgin steel fibers, which often entail higher costs and increased greenhouse emissions.

Regarding the manufacture of the reference mixture: the aggregates were heated to 180°C and the binder to 165°C. Then, the coarse and fine fraction was mixed with the asphalt binder and finally the filler fraction was added. The mixture was compacted according to the Marshall method with 50 blows on each side.

As for the experimental mixtures, aggregates and binder were heated up to 180°C and 165°C respectively, while the magnetic aggregate was not heated. Then, the coarse fraction was mixed with the asphalt binder and finally the fine fraction and the magnetic aggregate were added. The mixture was compacted according to the Marshall method with 50 blows on each side.

2.3. Research methodology

2.3.1. Determination of self-healing capacity

To determine the self-healing capacity, the asphalt mixtures under study were subjected to a cyclic rupture-healing-rupture test. For the first rupture, the samples were tested in flexure (Fig. 3). Thus, the reference and two experimental samples were conditioned with a 22.5 mm diameter cut (Fig. 3) and frozen at −20 °C for 48 h to induce brittle fracture (to ensure that the two resulting pieces are not deformed and could be re-bonded). Then, the healing process varied according to the type of mixture:

- The reference mixture was bonded and allowed to stand for 90 summer days in a room with daily temperature control. The objective was to get an order of magnitude of the self-healing capacity of the asphalt mixtures and to compare the effectiveness of healing by magnetic induction.
- The two experimental mixtures were healed by magnetic induction: a 300 A magnetic field was applied until different temperatures were reached (80°C, 90°C, 100°C, 110°C and 120°C). The magnetic induction was applied by means of a high frequency Easy Heat LI 3542 unit (Fig. 4). The magnetic induction coil was placed at a distance of 1 cm from the mixture, since varying the distance varies the heating efficiency [45–49]. The process was monitored in real time using an Optris PI Connect infrared thermal camera.

Table 2
Properties of natural aggregates.

Aggregate type	Property	Value	Limit	Standard
Ophite	Los Angeles coefficient	13	≤ 20	EN 1097–2
	Specific weight (g/cm^3)	2.787	-	EN 1097–6
	Polished stone value (PSV)	60	≥ 56	EN 1097–8
	Flakiness Index (%)	8	≤ 20	EN 933–3
Limestone	Los Angeles coefficient	28	-	EN 1097–2
	Specific weight (g/cm^3)	2.705	-	EN 1097–6
	Sand equivalent	78	> 55	EN 933–8
Hydrated lime	Specific weight (g/cm^3)	1.959	-	EN 1097–6

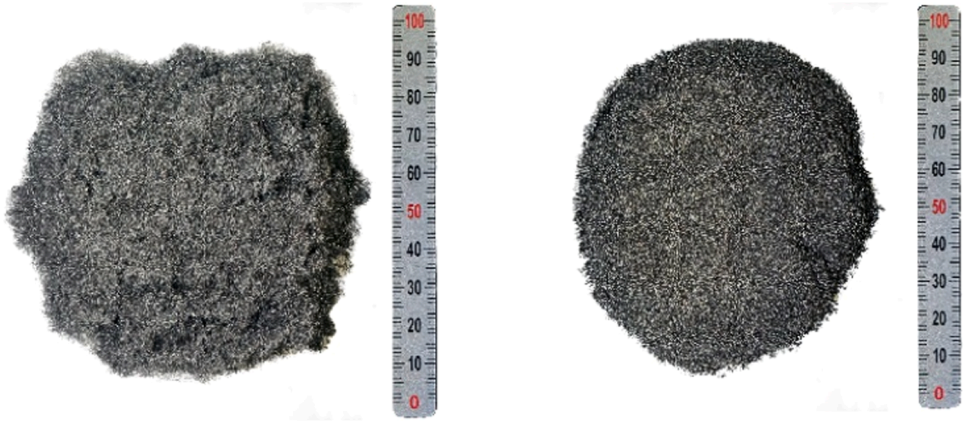

Fig. 1. Magnetic aggregate. Left: virgin steel fiber. Right: steel shot blasting.

Table 3
Detail of mixtures.

Mixture	Binder type	Binder content (%)	Magnetic Aggregate	Magnetic aggregate content (%)
Reference	PMB	4.5	No aggregate	-
Exp. 1	PMB	4.5	Virgin steel	1
Exp. 2	PMB	4.5	Steel shot blasting	1

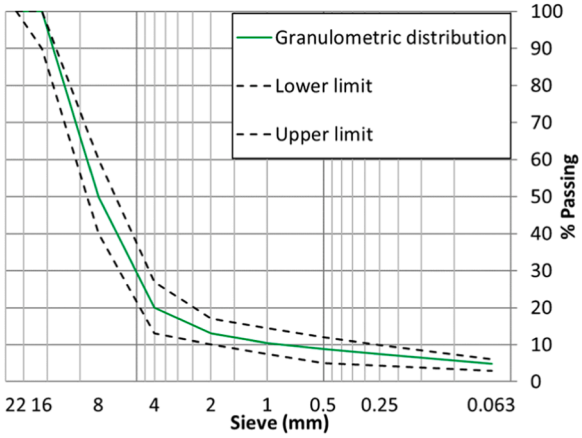

Fig. 2. Granulometric distribution.

After the healing process was completed, the specimens of all mixtures were left to stand for 2 h. They were then refrozen and tested to rupture in the flexural test.

Once the rupture-healing-rupture test was completed, the healing rate was determined using Eq. 1. The temperature that obtained the highest percentage of healing was selected as the healing temperature, which will be used to continue the investigation in the following sections.

$$\%healing = \frac{Remaining\ resistance}{Initial\ resistance} \cdot 100 \quad (1)$$

2.3.2. Particle loss with different healing cycles

Raveling is the main failure mode of porous asphalt mixtures [50, 51]. Despite the above, the actual impact of magnetic induction healing on particle loss is still unknown. In addition, the timing of the application of magnetic induction healing in asphalt mixtures is not known. For these reasons, in this section, different healing cycles were applied to the experimental mixtures in the Cantabro particle loss test and the particle loss by brushing test.

Firstly, the Cantabro test for particle loss was performed according to EN 12697–17. The test was carried out at 25°C. The particle loss was controlled every 50 revolutions. The experimental mixtures were tested to equal the particle loss of the reference mixture after 300 revolutions. To meet the objective of this section, the experimental samples were subjected to the healing cycles detailed in Table 4.

In addition, the brush particle loss test developed by [52] was carried out by applying different healing cycles: a steel brush scrapes the surface of the asphalt slabs at a frequency of 21 revolutions per minute with a load of 3.7 kg/cm^2. Particle loss was monitored every 250 revolutions. The experimental mixtures were tested to equal the particle loss of the

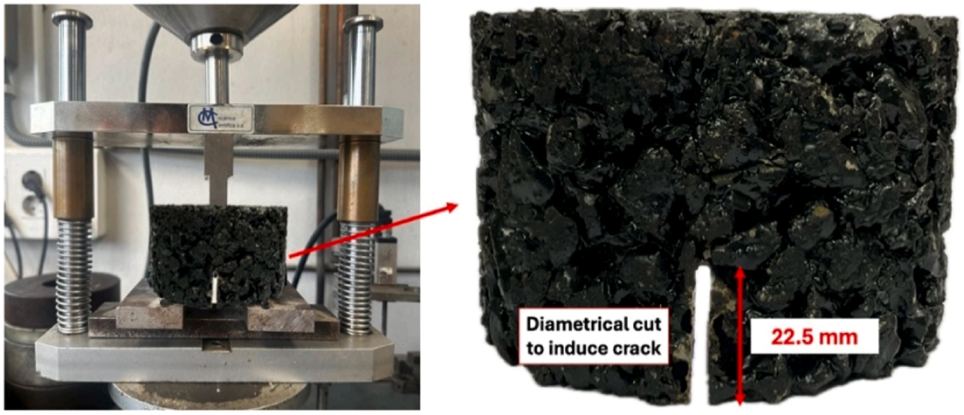

Fig. 3. Marshall sample with diametral cut.

Fig. 4. Magnetic induction machine setup.

Table 4
Healing detail of Cantabro test.

Type of mixture	Healing detail	Name
Reference	unhealed	Ref.
Exp. 1	unhealed	Exp. 1–00
	healed every 50 cycles	Exp. 1–50
	healed every 100 cycles	Exp. 1–100
	healed every 150 cycles	Exp. 1–150
Exp. 2	unhealed	Exp. 2–00
	healed every 50 cycles	Exp. 2–50
	healed every 100 cycles	Exp. 2–100
	healed every 150 cycles	Exp. 2–150

Table 5
Healing detail of brush particle loss test.

Type of mixture	Healing detail	Name
Reference	unhealed	Ref.
Exp. 1	unhealed	Exp. 1–00
	healed every 250 cycles	Exp. 1–250
	healed every 500 cycles	Exp. 1–500
Exp. 2	unhealed	Exp. 2–00
	healed every 250 cycles	Exp. 2–250
	healed every 500 cycles	Exp. 2–500

reference mixture after 1000 revolutions. The test setup is shown in Fig. 5. Like the cantabro test, different healing cycles were applied to the asphalt samples, what is summarized in Table 5.

2.3.3. *Rheological consequences of repeated healing on polymer modified bitumen*

Healing by magnetic induction can be reiterated [20–22]. However, previous research does not agree on the consequences of this thermal process on the binder. For this reason, in this section a rheological study is carried out on the binder of the newly manufactured reference mixture and on the binder of the experimental mixtures after 20 healing cycles.

Accordingly, the binder was recovered from the asphalt mixtures by rotary evaporation (EN 12697–3). The binder samples were then conditioned and tested for: softening temperature by the ring and ball test (EN 1427); penetration rate was determined by the needle method (EN 1426); viscosity, stiffness and phase angle were determined by the Dynamic shear rheometer (EN 14770) over a frequency range of 0.1 Hz to 30 Hz and temperatures from 30°C to 75°C.

Additionally, to characterize the binders independently from frequency and temperature, the master curves were determined considering the results obtained in DSR. The master curve is given by Eq. 2 [53].

$$\log(|G^*|) = \eta + \frac{\beta}{1 + e^{\gamma - \mu \log(f_r)}} \quad (MPa) \tag{2}$$

Where η is lower asymptote, γ and μ are shape parameters, f_r is frequency relative to temperature, β is the difference between the asymptote's values.

To evaluate the significance of the results, a statistical evaluation was performed using Minitab software with 95 % confidence interval: if the results were found to be parametric, t-Student was applied. On the contrary, U-mann Whitney was used.

Fig. 5. Brush particle loss test setup.

2.3.4. Functional consequences of repeated healing on porous asphalt mixtures

The main functional properties of porous mixtures are their ability to manage water runoff [54–57] and reduce traffic noise [58]. For this reason, interconnected voids, total voids, permeability and noise absorption were evaluated in this section at the initial state and after 5, 10, 15 and 20 healing cycles.

First, the total and interconnected voids were determined with Eqs. 3 and 4 according to EN 12697–8. Where, m_{dry} are the dry-weighted mass of the sample and V is the volume of the sample. G_{mm} is the maximum specific weight and m_{satw} is the mass of the saturated sample.

$$Total\ air\ voids(\%) = \left(1 - \frac{m_{dry}}{V \bullet G_{mm}}\right) \times 100 \quad (3)$$

$$Interconnected\ air\ voids(\%) = \left(\frac{V - \frac{m_{dry} - m_{satw}}{\rho_{water}}}{V}\right) \times 100 \quad (4)$$

Secondly, the permeability (mm/s) capacity was determined as the time it takes for a given volume of water to pass through a Marshall sample, according to Eq. 5. Where "L" is the depth and "A" is the cross-sectional area of sample, "a" represents the internal cross-sectional area of the tube, "t" is the time, and "h_1" and "h_2" represent the initial and final water heights. The test setup can be seen in the Fig. 6.

$$permeability\ in\ mm \Big/ s = \frac{aL}{At} \ln\left(\frac{h_1}{h_2}\right) \quad (5)$$

Finally, the noise absorption was determined using the impedance tube method (ISO 10534–2), the frequency of interest was below 1800 Hz [40] and the tube had a diameter of 100 mm. The absorption coefficient was determined by Eq. 6. Test setup can be seen in the Fig. 7.

$$Absorption\% = \frac{not - reflected\ energy}{incoming\ energy} \quad (6)$$

In the same way than in the previous section, a statistical evaluation was carried out using Minitab software with the same parameters.

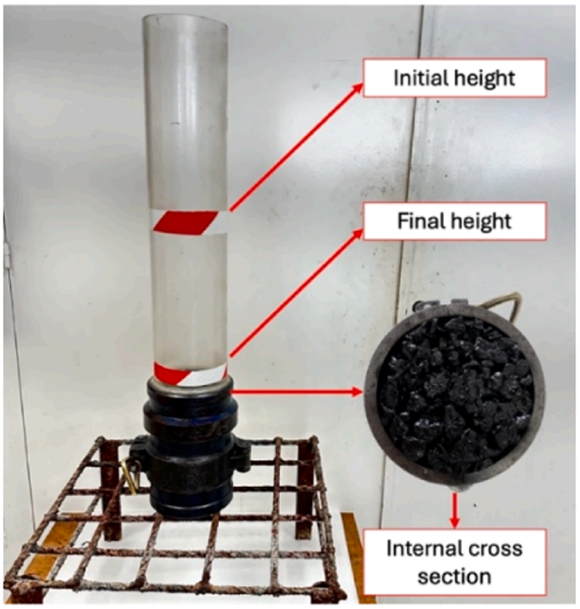

Fig. 6. Permeability test setup.

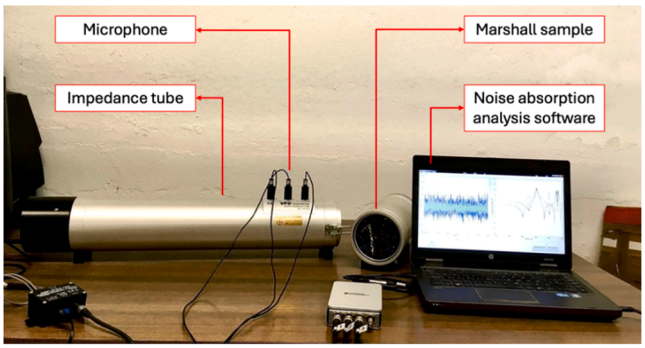

Fig. 7. Noise absorption test setup.

3. Results and discussion

3.1. Determination of healing capacity

The three studied asphalt mixtures had an equivalent percentage of voids (Table 6). Therefore, the influence of the internal structure on the healing capacity of the samples is discarded.

The first objective of this section is to test the self-healing capacity of the asphalt mixtures. In this respect, Fig. 8 shows the reference samples that were flexurally tested and then left at room temperature for 90 days with an average temperature of 25°C had a healing rate of about 20 %. In other words, the asphalt mixtures can heal on their own, unfortunately, the healing rate at room temperature is poor.

The second objective of this section was to determine the healing temperature for the following chapters. In this respect, it is possible to visualize in Fig. 8 that the optimum healing temperature seems to be 120°C. It has not been possible to completely heal the strength capacity of the experimental mixtures, what can be explained by the fact that the aggregates fracture in the flexural test, which after the healing process are bonded together by the binder which has less strength than the aggregate.

The self-healing performance between Exp 1 and Exp 2 show almost equivalent behaviour. This result makes sense since both contained the same asphalt binder and equivalent void content. Now, referring specifically to the 120°C target temperature, in Exp 1 the virgin steel fibers allowed the samples to reach the target temperature in only 50 s, whereas in Exp 2 the steel shot by-product allowed the samples to reach the target temperature in 3 min. However, virgin steel fibers take longer to cool than steel shot. For all the above, the use of the industrial by-product makes it possible to achieve the same percentage of self-healing, but to increase the time of application of the magnetic field.

Regarding general conclusions on the healing process, Fig. 8 shows an increase in self-healing as the temperature achieved in the healing process increases. However, it should be noted that there is an activation temperature at which the asphalt binder begins to expand and seal the cracks, since there is no significant difference between the healing achieved by the reference mixture and the mixtures exp 1 and exp 2 healed at 80°C. However, above 90°C, it is evident that the magnetic induction healing process is functional. Finally, it is important to note that when the optimal healing temperature is exceeded, the self-healing capacity decreases, possibly because the excess temperature generates a rearrangement of the particles and potential draindown of the binder.

Table 6
Density and total air voids of mixtures.

Mixture	Density (gr/cm^3)	Total voids (%)
Reference	2.777	24.6 ± 1.0
Exp. 1	2.810	24.7 ± 0.8
Exp. 2	2.983	24.4 ± 0.7

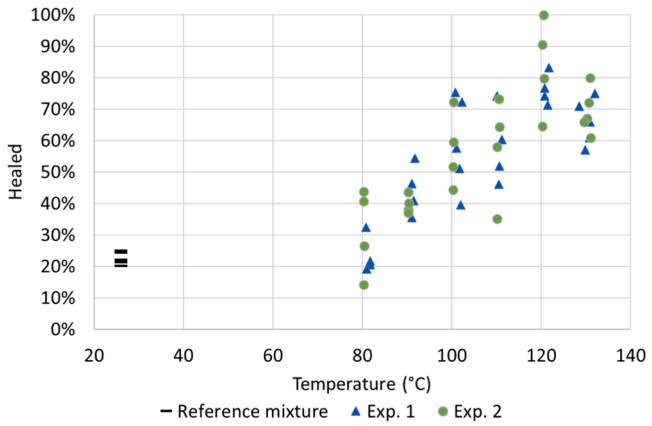

Fig. 8. Crack-heal-crack test results.

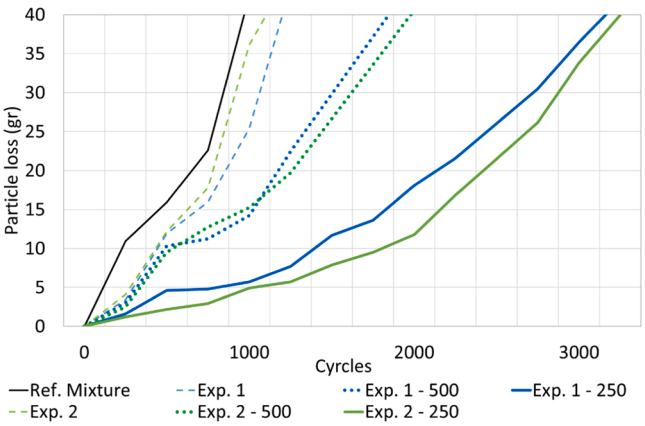

Fig. 10. Test results particle loss by brush.

3.2. Particle loss with different healing cycles in the cantabro test and loss of surface particles test

The objective of this section is to determine the impact of different healing cycles on the lifetime of the mixture with respect to particle loss. In this regard, in both tests (Fig. 9 and Fig. 10), it is evident that the application of magnetic induction healing cycles improves the performance of the mixtures compared to the mixtures that were not healed. In this sense, the mixtures in the cantabro test (Fig. 9) that were cured every 50 revolutions and the mixtures that were healed every 250 cycles in the particle loss by brush test (Fig. 10) showed a significant increase in performance against particle loss. This can be ascribed to the fact that an early age healing allows the healing of the micro cracks, preventing the formation of large cracks that allow the particles to detach.

In both tests (Fig. 9 and Fig. 10) it is evident that the performance of the mixtures with respect to particle loss is strongly influenced by the healing cycles, and not by the type of magnetic aggregate in the mixture. For this reason, it is possible to state that healing by magnetic induction is equally effective irrespectively of the use of virgin steel fiber or the industrial by-product used in this research. In addition, the asphalt mixtures with the same healing cycles performed equally well in terms of particle loss.

All samples that had healing cycles showed higher resistance against ravelling in comparison to the samples that were not healed. Specifically, in Fig. 9, the mixtures healed every 50 revolutions (Exp. 1–50 and Exp. 2–50) achieved 10 % particle loss between 900 and 1000 revolutions, thus reducing to a third the particle loss shown by the experimental mixtures without healing (Exp. 1 and Exp. 2) which had the same percentage loss after 300 revolutions. Similarly, in Fig. 10 the mixtures healed every 250 cycles (Exp. 1–250 and Exp. 2–250) also reduced to a third the loss of particles in comparison to the reference mixture and experimental mixtures with no healing cycles. In this sense, it is possible to state that healing by magnetic induction at early ages of the asphalt mixtures is able to reduce the loss of particles to a third, significantly improving their performance in terms of ravelling.

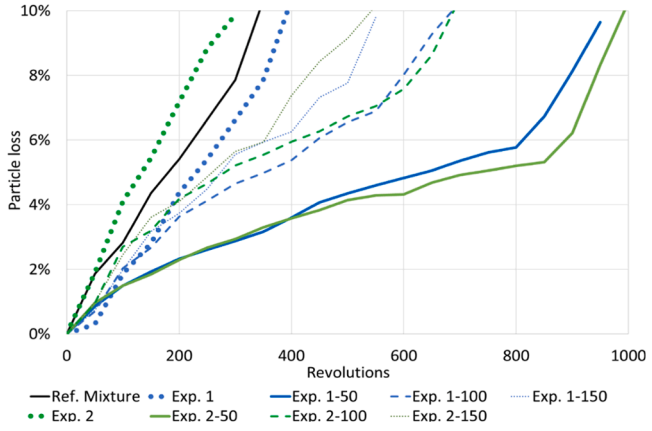

Fig. 9. Cantabro test results.

3.3. Rheological consequences of repeated healing on polymer modified bitumen

To increase the durability of the experimental mixtures, the healing process had to be repeated. In this sense, the thermal process of healing by magnetic induction may or may not have consequences on the asphalt binder. For this reason, the objective of this section is to conclude the rheological impact of repeated healing cycles. For this purpose, the asphalt binder of the reference mixture recovered immediately after manufacture was compared with the asphalt binder recovered from Exp. 1 and Exp. 2 after 20 healing cycles.

The residual binders of Exp. 1 and Exp. 2 had a slight increase in softening point (Table 7). However, the slight increase is not statistically significantly different from the residual binder of the reference mixture without healing cycles (Table 8). In addition to the above, the residual binders of Exp. 1 and Exp. 2 decreased the degree of penetration, being this result statistically significant, so that the application of healing cycles increases the hardness of the asphalt binders type PMB 45/80–65. Now, when comparing the results of the residual binders of the two experimental mixtures, Exp. 1 presents a slightly higher softening temperature than Exp. 2, which is not statistically significant. On the other hand, in the penetration test, Exp. 1 shows a statistically higher hardness than Exp. 2 after 20 healing cycles. This could be due, as mentioned in the previous chapter, to the fact that virgin steel fibers have different heating and cooling times than the industrial byproduct, so that Exp. 1 was exposed to high temperatures for longer than Exp. 2.

The residual binders of Exp. 1 and Exp. 2 have a slightly higher viscosity than the residual binder of the reference mixture without healing (Fig. 11). However, this slight increase is not statistically significant (Table 9). In particular, the residual binder of Exp. 2 had a viscosity intermediate to that exhibited by the residual binder of Exp. 1 and the reference mixture. Based on the statistical analysis, the healing cycles do not significantly affect the viscosity grade of PMB 45/80–65 type asphalt binders, possibly because the healing cycles have a very

Table 7
Ring and ball and penetration test results.

Mixture	Binder type	Softening point (°C)	Penetration (mm)
Reference	PMB 45/80–65	72.3 ± 1.7	40.1 ± 1.5
Exp. 1	PMB 45/80–65	79.1 ± 0.4	29.9 ± 1.1
Exp. 2	PMB 45/80–65	75.8 ± 1.6	31.9 ± 0.6

Table 8
P-value Ring and ball and penetration test.

Residual bitumen	P-value			
	Ring and ball	Status	Penetration	Status
Ref. Mixture - Exp. 1	0.2453	Not significant	0.0195	Significant
Ref. Mixture - Exp. 2	0.2453	Not significant	0.0139	Significant
Exp. 1 - Exp. 2	0.2453	Not significant	0.0000	Significant

short duration and the temperatures reached are lower than those recommended by the manufacturer for the binder to start draining.

The stiffness of the residual binders of the experimental mixtures and the reference mixture do not show a statistically significant difference (Fig. 12 and Table 10), so the experimental mixtures should not be more affected by cracking than the reference mixture. Again, the residual binder of Exp. 2 again showed an intermediate performance between the reference mixture and Exp. 1. In this sense, it seems that the binder of Exp. 1 has been more affected by thermal processes than the residual binder of Exp. 2 containing steel shot blasting. However, the consequences on the stiffness of the binder type PMB 45–80/65 per healing cycle are negligible considering that after 20 healing cycles the differences are not statistically significant.

The phase angle of the residual binder of the reference mixture does not show statistically significant differences with the residual binder of the experimental mixtures after 20 healing cycles (Fig. 13 and Table 11). In this regard, it is important to note that the Exp. 2 residual binder again had an intermediate performance, with the Exp. 1 residual binder having the lowest phase angle. This result is in agreement with the performance exhibited by the residual binders studied with respect to ring and ball, penetration, viscosity and stiffness.

The master curve confirms the results discussed up to this point (Fig. 14). There are no statistically significant differences with respect to the performance of the residual binders of the reference mixture without healing cycles and the residual binder of Exp. 1 and Exp. 2 after 20

Table 9
P-value Dynamic shear rheometer: viscosity.

Residual bitumen	P-value	
	Viscosity	Status
Ref. Mixture - Exp. 1	0.3075	Not significant
Ref. Mixture - Exp. 2	0.7337	Not significant
Exp. 1 - Exp. 2	0.7337	Not significant

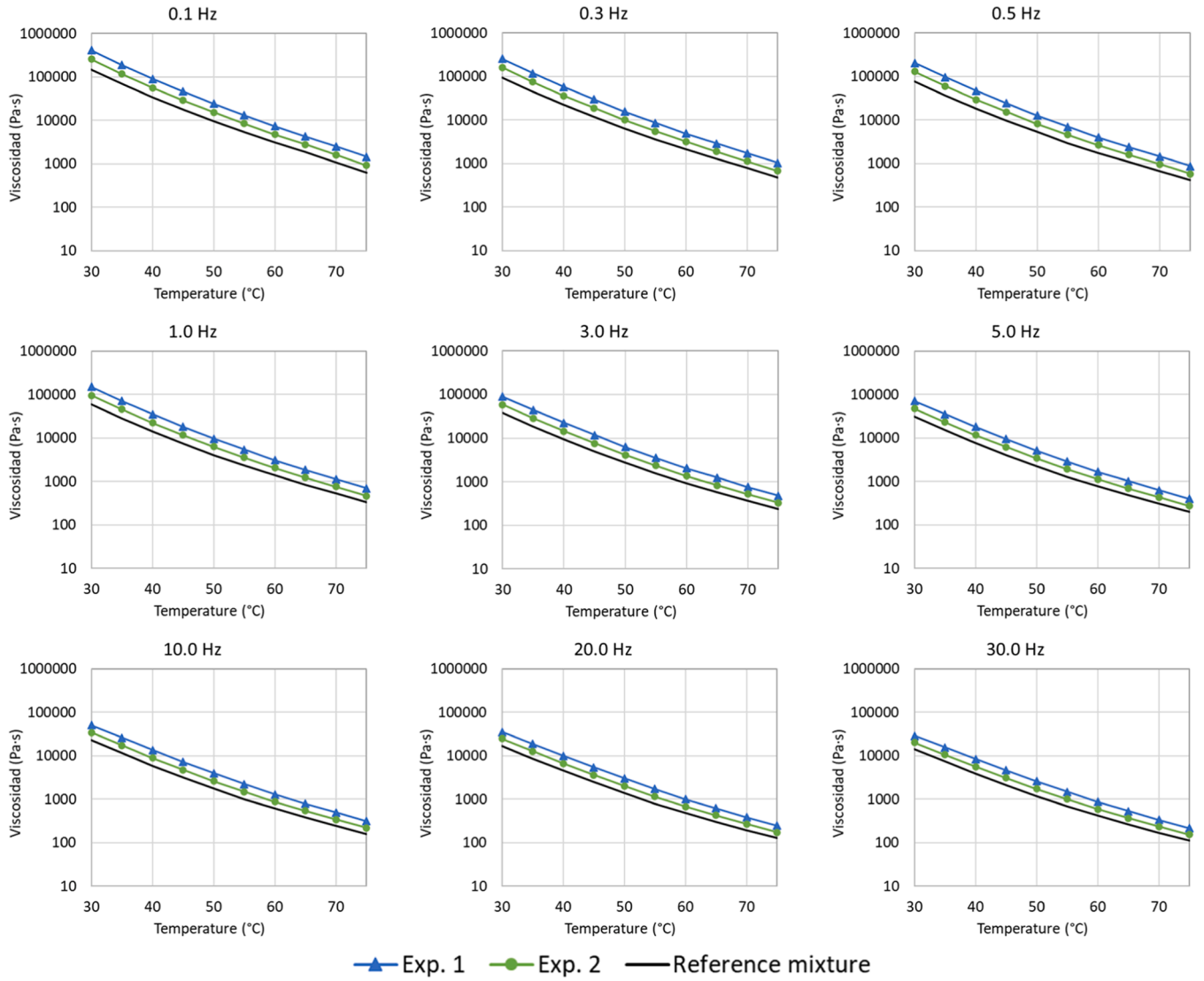

Fig. 11. Dynamic shear rheometer test results: viscosity.

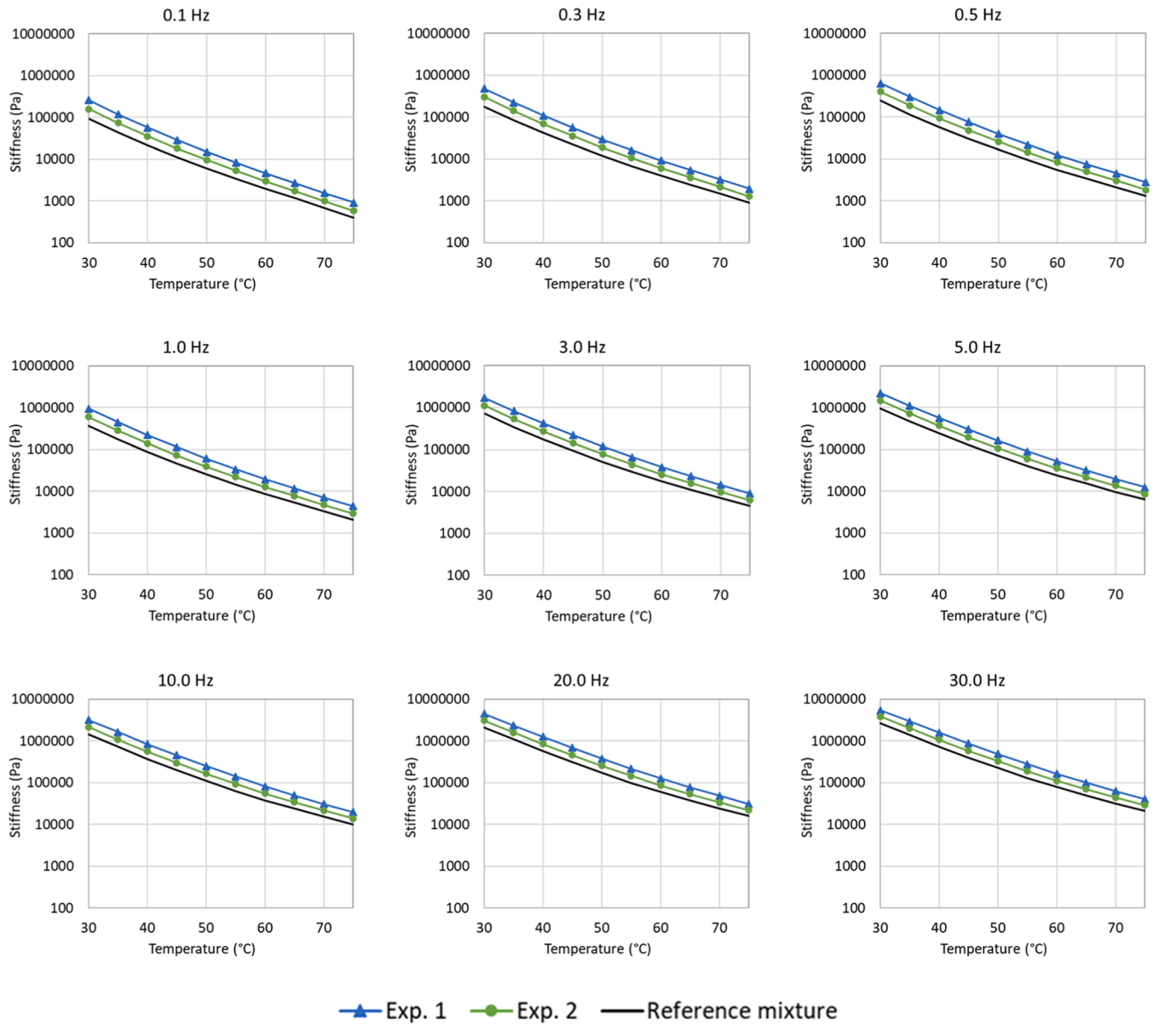

Fig. 12. Dynamic shear Rheometer test results: stiffness.

Table 10
P-value dynamic shear rheometer: stiffness.

Residual bitumen	P-value	
	Stiffness	Status
Ref. Mixture - Exp. 1	0.163	Not significant
Ref. Mixture - Exp. 2	0.457	Not significant
Exp. 1 - Exp. 2	0.415	Not significant

healing cycles (Table 12). However, the master curves show the same trend as in the ring and ball, penetration and DSR tests: the binder of Exp. 2 has an intermediate performance between Exp. 1 and the reference mixture. In this sense, it seems that the healing process by means of magnetic induction produces a minimum degradation to the binder. This is because although there are no statistically significant differences, an increase in the hardness of the binder after 20 cycles of healing is observed, especially in Exp. 1, which can be explained by the fact that the virgin steel fibers take longer to cool down, so the thermal process is longer than in Exp. 2.

Based on the above, there appears to be very little ageing and in many of the properties it is not significant, so it can be said that its impact is far from the caused, for example, by the ageing of the mixtures due to climatic conditions.

3.4. Functional consequences of repeated healing on porous asphalt mixtures

The objective of this section is to determine the implications of repeated healing cycles with respect to their permeability and noise absorption capacity. In this regard, it is evident from Fig. 15 that the total number of voids in the mixtures is not affected by repeated healing cycles. On the other hand, the interconnected voids do show a slight decrease, however, this variation is not statistically significant (Table 13). This result can be explained by the fact that since the temperature of the binder is increased by magnetic induction, there is a slight run-off of the binder towards the bottom of the asphalt mixture, so that the interconnected voids are slightly reduced and the total voids stay constant because the material is the same.

Fig. 16 shows a slight decrease in the permeability of the

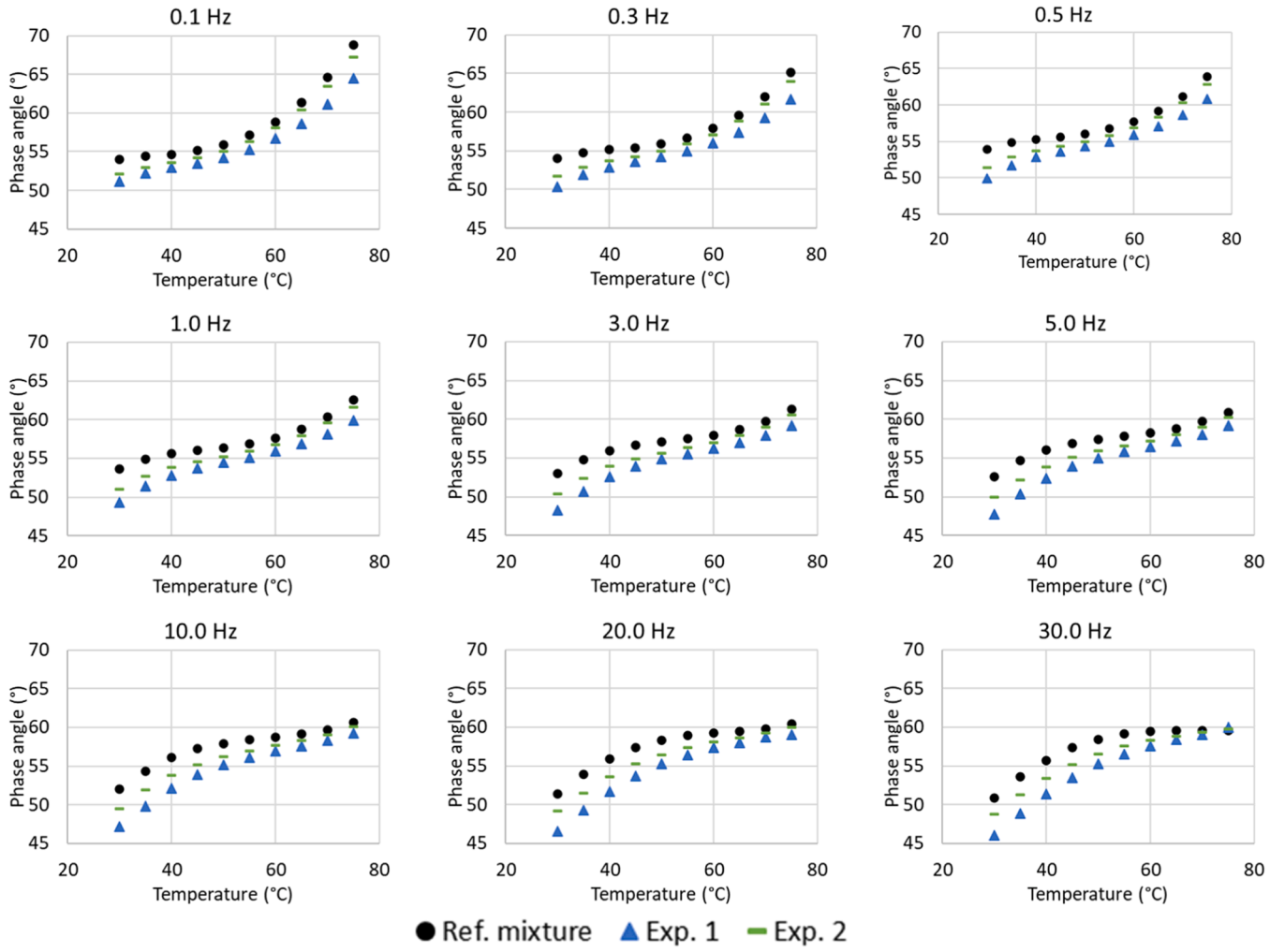

Fig. 13. Dynamic shear rheometer test results: phase angle.

Table 11
P-value dynamic shear rheometer: phase angle.

Residual bitumen	P-value	
	Phase angle	Status
Ref. Mixture - Exp. 1	0.064	Not significant
Ref. Mixture - Exp. 2	0.279	Not significant
Exp. 1 - Exp. 2	0.426	Not significant

experimental mixtures due to repeated healing cycles. Importantly, this slight decrease is not statistically significant (Table 14). However, although the slight decrease in permeability is not statistically significant, it does point to a small decrease in the permeability of the asphalt mixture after each healing cycle. In this sense, the slight decrease that occurs can be explained by the slight decrease in the interconnected voids due to the slight runoff produced by the increase in the temperature of the mixtures in each healing cycle.

At the same time, Fig. 17 shows that the healing cycles increase the noise absorption capacity of the asphalt mixture, and this variation is statistically significant independent of the type of magnetic aggregate used (Table 14). In this sense, the significant increase in the absorption coefficient can be explained again by the slight drain down to the bottom of the sample of the asphalt mixture due to the increase in temperature. This slight drain down to the bottom of the sample probably increases the porosity at the top of the mixtures, which contributes to an increase in the noise absorption capacity of the mixture. Specifically, the

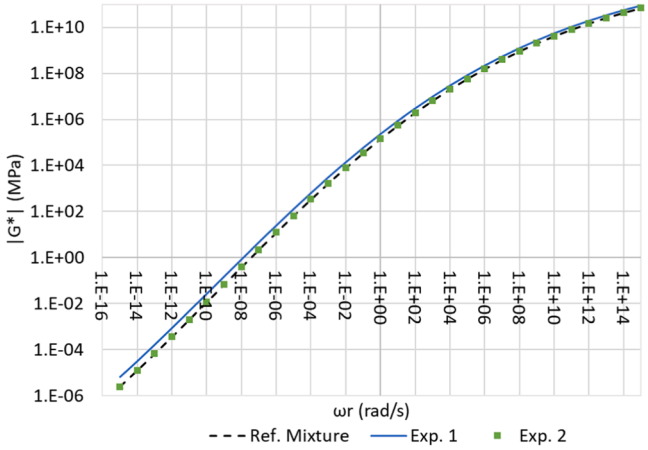

Fig. 14. Master curves.

experimental mixtures have a statistically significant higher absorption than the reference mixture.

4. Conclusions

In this study, the impact of different healing cycles on the particle loss of two experimental porous asphalt mixtures made with PMB

Table 12
P-value Master curve.

Residual bitumen	P-value	
	Phase angle	Status
Ref. Mixture – Exp. 1	0.762	Not significant
Ref. Mixture – Exp. 2	0.423	Not significant
Exp. 1 – Exp. 2	0.540	Not significant

40–80/65 asphalt binder was evaluated. Therefore, the healing cycles were repeated in order to clarify the impact of this on the residual binder and on the functional properties of the asphalt mixture, in particular with regard to its permeability and noise absorption. In this respect, it is possible to conclude that:

- Self-healing of porous asphalt mixtures is poor at room temperature. Reference mixtures healed at room temperature achieved a 20 % healing rate after 90 days. Magnetic induction is required as far as the process needs to be accelerated.
- Magnetic induction healing of porous asphalt mixtures is able to reduce particle loss to a third if it is applied several times, which significantly improves the performance over ravelling. This can be ascribed to the fact that the healing allows micro-cracks to heal, preventing the formation of large cracks that would allow the detachment of the particles. Furthermore, this result is obtained irrespective of the use of virgin steel fibres or industrial by-products.
- There is a healing activation temperature at which the asphalt binder starts to expand and seal the cracks. This is supported by the fact that there is no difference between the healing achieved by the reference mixture and the mixtures exp 1 and exp 2 healed at 80°C. However, above 90°C it is evident that the magnetic induction healing process is functional.
- There are no statistically significant differences regarding the performance of the residual binders of the reference mixture without healing cycles and the residual binder of Exp. 1 and Exp. 2 after 20 healing cycles. On the other hand, it seems that the healing process using magnetic induction produces minimal degradation of the binder, since despite there are no statistically significant differences, an increase in the binder hardness is seen after 20 healing cycles, especially in Exp 1, which can be explained by the fact that virgin steel fibres take longer to cool, so the thermal process is longer than in Exp. 2.
- Repeating the healing cycles 20 times produces a slight decrease in the interconnected voids due to the slight drainage produced by the increase in the temperature of the mixtures in each healing cycle. This produces a slight decrease in permeable capacity that is not statistically significant. Therefore, the porous mixtures

Table 13
P-value total voids and interconnected voids.

Mixture	P-value			
	Total voids	Status	Interconnected voids	Status
Ref. - Exp. 1	0.750	Not significant	0.525	Not significant
Ref. - Exp. 2	0.241	Not significant	0.283	Not significant
Exp. 1 - Exp. 2	0.944	Not significant	0.194	Not significant

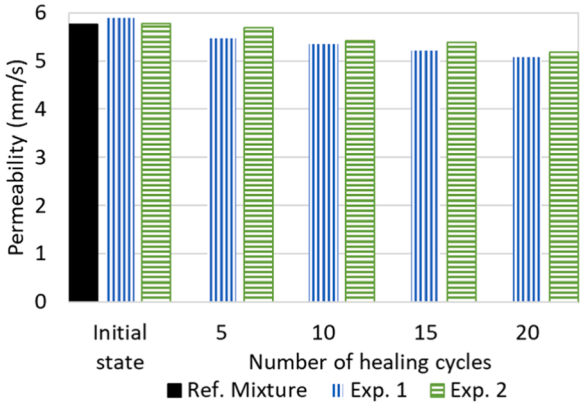

Fig. 16. Permeability test results.

Table 14
P-value permeability and absorption.

Mixture	P-value			
	Permeability	Status	Absorption	Status
Ref. Mixture - Exp. 1 Initial	0.796	Not significant	0.000	Significant
Ref. Mixture - Exp. 2 Initial	0.994	Not significant	0.000	Significant
Exp. 1 Initial - Exp. 2 Initial	0.885	Not significant	0.000	Significant
Exp. 1 Initial - Exp. 1 Final	0.172	Not significant	0.000	Significant
Exp. 2 Initial - Exp. 2 Final	0.666	Not significant	0.023	Significant

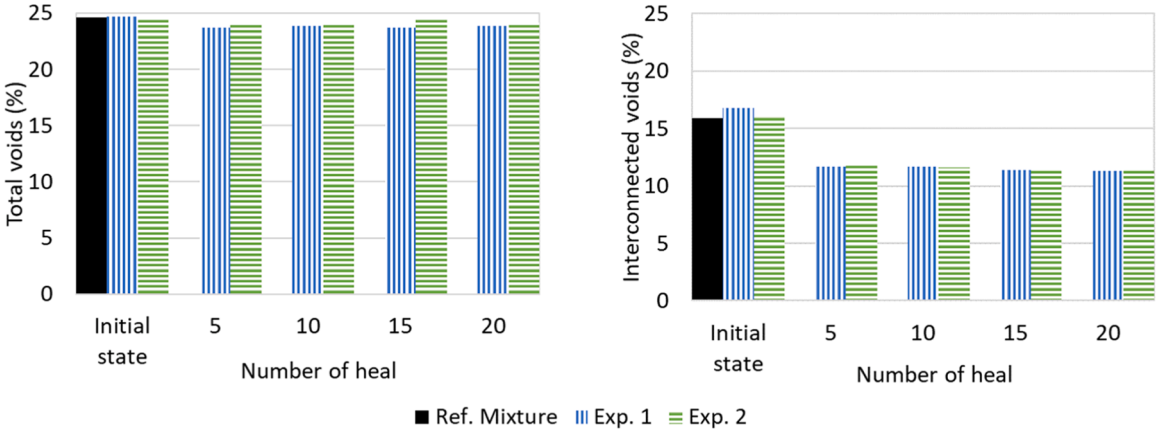

Fig. 15. Total voids and interconnected voids.

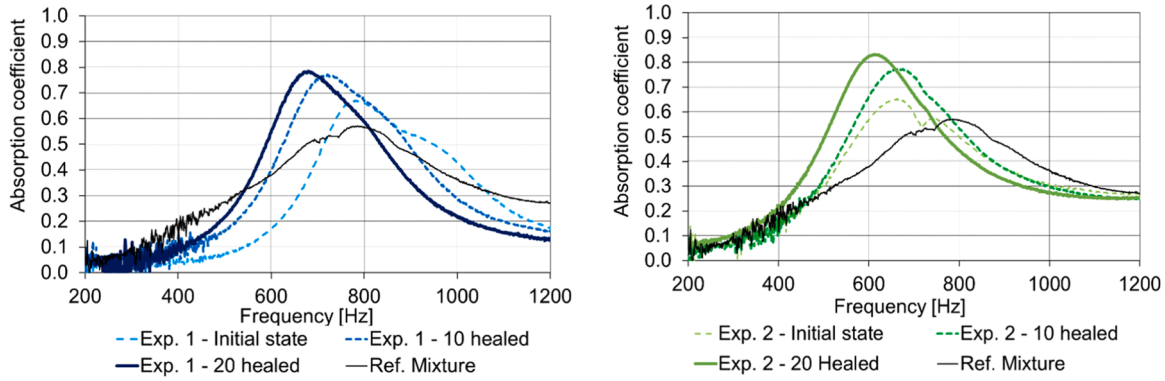

Fig. 17. Absorption test results.

manufactured with PMB 45–80/65 binder are not negatively affected by the healing cycles in terms of permeability.

– The repetition of the healing cycles increases the noise absorption capacity of the asphalt mixture; this variation is statistically significant regardless of the type of magnetic aggregate used. In this sense, the significant increase in the absorption coefficient can again be explained by a slight run-off of the binder which probably increases the porosity in the upper part of the mixtures.

The self-healing capacity of asphalt pavements is very slow and inefficient. In this sense, magnetic induction technology has very favorable results regarding the loss of particles and a low degree of consequences with respect to the rheology of the binder and the functional properties of the mixture. In the future, to make the technology viable at a real scale, work must be done on optimizing magnetic induction equipment to be able to scale this technology in an environmentally and economically efficient way.

CRediT authorship contribution statement

Christopher Delafuente-Navarro: Writing – review & editing, Writing – original draft, Visualization, Methodology, Investigation, Formal analysis, Conceptualization. **Pedro Lastra-González:** Writing – review & editing, Visualization, Validation, Supervision, Formal analysis, Data curation, Conceptualization. **Irune Indacoechea-Vega:** Writing – review & editing, Validation, Supervision, Project administration, Formal analysis, Data curation. **Daniel Castro-Fresno:** Writing – review & editing, Resources, Project administration, Funding acquisition, Data curation, Conceptualization.

Declaration of Competing Interest

The authors declare that they have no known competing financial interests or personal relationships that could have appeared to influence the work reported in this paper.

Acknowledgements

This publication is part of the project SICA + (Ref. PDC2021–120824-I00), financed by MICIU/AEI/10.13039/501100011033 and by the European Union Next Generation EU/PRTR. The authors acknowledge and thank these institutions.

The authors would like to thank José Maria Moreno Rodríguez and María Del Mar Colás of Cepsa Comercial Petróleo S.A. for their collaboration. At the same time, we thank Paula Del Rio Gandarillas, Maria Teresa Rodriguez Valero and Andrés Rivas Sánchez, whose excellent work in the laboratory gave a fundamental added- value to the development of this research.

Data Availability

Data will be made available on request.

References

[1] B.R. Anupam, U.C. Sahoo, A.K. Chandrappa, A methodological review on self-healing asphalt pavements, Constr. Build. Mater. 321 (2022) 126395, https://doi.org/10.1016/j.conbuildmat.2022.126395.

[2] D. Sun, et al., A comprehensive review on self-healing of asphalt materials: mechanism, model, characterization and enhancement, Adv. Colloid Interface Sci. 256 (2018) 65–93, https://doi.org/10.1016/j.cis.2018.05.003.

[3] P. Ayar, F. Moreno-Navarro, M.C. Rubio-Gámez, The healing capability of asphalt pavements: a state of the art review, J. Clean. Prod. 113 (2016) 28–40, https://doi.org/10.1016/j.jclepro.2015.12.034.

[4] E. Schlangen, S. Sangadji, Addressing infrastructure durability and sustainability by self healing mechanisms - recent advances in self healing concrete and asphalt, Procedia Eng. 54 (2013) 39–57, https://doi.org/10.1016/j.proeng.2013.03.005.

[5] J.M. Yang, J.K. Kim, D.Y. Yoo, Effects of amorphous metallic fibers on the properties of asphalt concrete, Constr. Build. Mater. 128 (2016) 176–184, https://doi.org/10.1016/j.conbuildmat.2016.10.082.

[6] L. Zhang, I. Hoff, X. Zhang, J. Liu, and C. Yang, A Methodological Review on Development of Crack Healing Technologies of Asphalt Pavement., 2023, doi: doi.org/10.3390/su15129659.

[7] J. Norambuena-Contreras, A. Garcia, Self-healing of asphalt mixture by microwave and induction heating, Mater. Des. 106 (2016) 404–414, https://doi.org/10.1016/j.matdes.2016.05.095.

[8] B. Liang, F. Lan, K. Shi, G. Qian, Z. Liu, J. Zheng, Review on the self-healing of asphalt materials: mechanism, affecting factors, assessments and improvements, Constr. Build. Mater. 266 (2021) 120453, https://doi.org/10.1016/j.conbuildmat.2020.120453.

[9] I. Pérez, B. Gómez-Meijide, A.R. Pasandín, A. García, G. Airey, Enhancement of curing properties of cold in-place recycling asphalt mixtures by induction heating, Int. J. Pavement Eng. 22 (3) (2021) 355–368, https://doi.org/10.1080/10298436.2019.1609674.

[10] A. Garcia-hernandez, Q. Liu, E. Schlangen, and M. Van De Ven, Unravelling of Porous Asphalt, Self Healing Materials: Pioneering Research in the Netherlands, pp. 159–164, 2015, doi: DOI10.3233/978-1-61499-514-2-159.

[11] C. Delafuente-navarro, P. Lastra-gonzález, I. Indacoechea-vega, and D. Castro-fresno, Healing by Magnetic Induction of A Novel Cold Pavement with Asphalt Emulsion and Industrial By-products., no. December 2023, 2024, doi: 10.1016/j.dibe.2024.100417.

[12] L.C. Aragão, et al., Extending the service life of asphalt concrete pavements through the addition of conductive metallic waste particles for induced crack healing, Aust. J. Civ. Eng. 19 (1) (2020) 1–14, https://doi.org/10.1080/14488353.2020.1795566.

[13] P. Lastra-González, I. Indacoechea-Vega, M.A. Calzada-Pérez, Á. Vega-Zamanillo, D. Castro-Fresno, Assessment of induction heating in the performance of porous asphalt mixtures, Road. Mater. Pavement Des. 21 (8) (2020) 2302–2320, https://doi.org/10.1080/14680629.2019.1606729.

[14] Q. Liu, Á. García, E. Schlangen, M. Van, De Ven, Induction healing of asphalt mastic and porous asphalt concrete, Constr. Build. Mater. 25 (9) (2011) 3746–3752, https://doi.org/10.1016/j.conbuildmat.2011.04.016.

[15] Q. Liu, E. Schlangen, M. Van De Ven, G. Van Bochove, J. Van Montfort, Evaluation of the induction healing effect of porous asphalt concrete through four point bending fatigue test, Constr. Build. Mater. 29 (2011) 403–409, https://doi.org/10.1016/j.conbuildmat.2011.10.058.

[16] A. Menozzi, A. Garcia, M.N. Partl, G. Tebaldi, P. Schuetz, Induction healing of fatigue damage in asphalt test samples, Constr. Build. Mater. 74 (2015) 162–168, https://doi.org/10.1016/j.conbuildmat.2014.10.034.

[17] A. García, M. Bueno, J. Norambuena-Contreras, M.N. Partl, Induction healing of dense asphalt concrete, Constr. Build. Mater. 49 (2013) 1–7, https://doi.org/10.1016/j.conbuildmat.2013.07.105.

[18] Y. Pamulapati, M.A. Elseifi, S.B. Cooper, L.N. Mohammad, O. Elbagalati, Evaluation of self-healing of asphalt concrete through induction heating and metallic fibers, Constr. Build. Mater. 146 (2017) 66–75, https://doi.org/10.1016/j.conbuildmat.2017.04.064.
[19] Q. Liu, W. Yu, E. Schlangen, G. Van Bochove, Unravelling porous asphalt concrete with induction heating, Constr. Build. Mater. 71 (2014) 152–157, https://doi.org/10.1016/j.conbuildmat.2014.08.048.
[20] Q. Dai, Z. Wang, M.R. Mohd Hasan, Investigation of induction healing effects on electrically conductive asphalt mastic and asphalt concrete beams through fracture-healing tests, Constr. Build. Mater. 49 (2013) 729–737, https://doi.org/10.1016/j.conbuildmat.2013.08.089.
[21] A. Tabaković, E. Schlangen, Self-Healing Technology for Asphalt Pavements. Advances in Polymer Science, Springer New York LLC, 2016, pp. 285–306, 27310, 1007/12_2015_335.
[22] E. Yalcin, Effects of microwave and induction heating on the mechanical and self-healing characteristics of the asphalt mixtures containing waste metal, Constr. Build. Mater. 286 (2021) 122965, https://doi.org/10.1016/j.conbuildmat.2021.122965.
[23] T.M. Phan, T.H.M. Le, D.W. Park, Evaluation of cracking resistance of healed warm mix asphalt based on air-void and binder content, Road. Mater. Pavement Des. 23 (1) (2022) 47–61, https://doi.org/10.1080/14680629.2020.1829010.
[24] Á. García, E. Schlangen, M. Van De Ven, D. Van Vliet, Induction heating of mastic containing conductive fibers and fillers, Mater. Struct. /Mater. Et. Constr. 44 (2) (2011) 499–508, https://doi.org/10.1617/s11527-010-9644-2.
[25] S. Xu, X. Liu, A. Tabaković, E. Schlangen, A novel self-healing system: towards a sustainable porous asphalt, J. Clean. Prod. 259 (2020), https://doi.org/10.1016/j.jclepro.2020.120815.
[26] J. Qiu, M.F.C. Van De Ven, S. Wu, J. Yu, A.A.A. Molenaar, Investigating the self healing capability of bituminous binders, Road. Mater. Pavement Des. 10 (2009) 81–94, https://doi.org/10.3166/RMPD.10HS.81-94.
[27] A.A.A. Molenaar, E.T. Hagos, M.F.C. van de Ven, Effects of aging on the mechanical characteristics of bituminous binders in PAC, J. Mater. Civ. Eng. 22 (8) (2010) 779–787, https://doi.org/10.1061/(asce)mt.1943-5533.0000021.
[28] E. Jeoffroy, F. Bouville, M. Bueno, A.R. Studart, M.N. Partl, Iron-based particles for the magnetically-triggered crack healing of bituminous materials, Constr. Build. Mater. 164 (2018) 775–782, https://doi.org/10.1016/j.conbuildmat.2017.12.223.
[29] Q. Liu, W. Yu, S. Wu, E. Schlangen, P. Pan, A comparative study of the induction healing behaviors of hot and warm mix asphalt, Constr. Build. Mater. 144 (2017) 663–670, https://doi.org/10.1016/j.conbuildmat.2017.03.195.
[30] C. Yang, et al., Enhanced induction heating and self-healing performance of recycled asphalt mixtures by incorporating steel slag, J. Clean. Prod. 366 (2022), https://doi.org/10.1016/j.jclepro.2022.132999.
[31] H. Ajam, B. Gómez-Meijide, I. Artamendi, A. Garcia, Mechanical and healing properties of asphalt mixes reinforced with different types of waste and commercial metal particles, J. Clean. Prod. 192 (2018) 138–150, https://doi.org/10.1016/j.jclepro.2018.04.262.
[32] Á. García, E. Schlangen, M. van de Ven, Q. Liu, Electrical conductivity of asphalt mortar containing conductive fibers and fillers, Constr. Build. Mater. 23 (10) (2009) 3175–3181, https://doi.org/10.1016/j.conbuildmat.2009.06.014.
[33] K. Liu, D. Dai, C. Fu, W. Li, S. Li, Induction heating of asphalt mixtures with waste steel shavings, Constr. Build. Mater. 234 (2020) 117368, https://doi.org/10.1016/j.conbuildmat.2019.117368.
[34] A. García, J. Norambuena-Contreras, M.N. Partl, P. Schuetz, Uniformity and mechanical properties of dense asphalt concrete with steel wool fibers, Constr. Build. Mater. 43 (2013) 107–117, https://doi.org/10.1016/j.conbuildmat.2013.01.030.
[35] T. James, D. Watson, A. Taylor, N. Tran, C. Rodezno, Improving cohesiveness of porous friction course (PFC) asphalt mixtures, Asph. Paving Technol. Assoc. Asph. Paving Technol. Proc. Tech. Sess. 86 (2017) 351–375, https://doi.org/10.1080/14680629.2017.1389073.
[36] M.A. Hernandez-Saenz, S. Caro, E. Arámbula-Mercado, A. Epps Martin, Mix design, performance and maintenance of Permeable friction courses (PFC) in the United States: state of the art, Constr. Build. Mater. 111 (2016) 358–367, https://doi.org/10.1016/j.conbuildmat.2016.02.053.
[37] A. de F. Smit, J.A. Prozzi, Quantification of the reduction of wet weather accidents using Porous friction courses (PFC), Procedia Soc. Behav. Sci. 96 (2013) 2745–2755, https://doi.org/10.1016/j.sbspro.2013.08.308.
[38] N.A. Valinski, D.G. Chandler, Infiltration performance of engineered surfaces commonly used for distributed stormwater management, J. Environ. Manag. 160 (2015) 297–305, https://doi.org/10.1016/j.jenvman.2015.06.032.
[39] A.E. Alvarez, E.M. Fernandez, A. Epps Martin, O.J. Reyes, G.S. Simate, L. F. Walubita, Comparison of permeable friction course mixtures fabricated using asphalt rubber and performance-grade asphalt binders, Constr. Build. Mater. 28 (1) (2012) 427–436, https://doi.org/10.1016/j.conbuildmat.2011.08.085.
[40] D. Castro-Fresno, H. Miera-Dominguez, P. Lastra-González, I. Indacoechea-Vega, R. van Loon, G. van Blokland, Two-layer porous asphalt: main properties to decrease the noise emissions, Transp. Res Rec. (2023), https://doi.org/10.1177/03611981231203231.
[41] H. Miera-Dominguez, et al., Design and validation of a new asphalt mixture to reduce road traffic noise pollution in urban areas, Case Stud. Constr. Mater. 20 (Jul. 2024) e03107, https://doi.org/10.1016/j.cscm.2024.e03107.
[42] P.R. Donavan, Effect of porous pavement on wayside traffic noise levels, Transp. Res Rec. 2403 (2014) 28–36, https://doi.org/10.3141/2403-04.
[43] R. Elvik, P. Greibe, Road safety effects of porous asphalt: a systematic review of evaluation studies, Accid. Anal. Prev. 37 (3) (2005) 515–522, https://doi.org/10.1016/j.aap.2005.01.003.
[44] F. Moreno-Navarro, M. Sol-Sánchez, M.C. Rubio-Gámez, The effect of polymer modified binders on the long-term performance of bituminous mixtures: the influence of temperature, Mater. Des. 78 (Aug. 2015) 5–11, https://doi.org/10.1016/j.matdes.2015.04.018.
[45] C. DeLaFuente-Navarro, P. Lastra-González, M.Á. Calzada-Pérez, D. Castro-Fresno, Rheological and mechanical consequences of reducing the curing time of cold asphalt mixtures by means of magnetic induction, Case Stud. Constr. Mater. (2023), https://doi.org/10.1016/j.cscm.2023.e02573.
[46] Á. García, E. Schlangen, M. Van De Ven, Q. Liu, A simple model to define induction heating in asphalt mastic, Constr. Build. Mater. 31 (2012) 38–46, https://doi.org/10.1016/j.conbuildmat.2011.12.046.
[47] C. Fu, F. Wang, K. Liu, Q. Liu, P. Liu, M. Oeser, Inductive asphalt pavement layers for improving electromagnetic heating performance, Int. J. Pavement Eng. 24 (1) (2023), https://doi.org/10.1080/10298436.2022.2159401.
[48] C. Fu, K. Liu, P. Liu, M. Oeser, Experimental and numerical investigation of magnetic converge effect of magnetically conductive asphalt mixture, Constr. Build. Mater. 360 (2022) 129626, https://doi.org/10.1016/j.conbuildmat.2022.129626.
[49] H. Xu, et al., Research on gradient characteristics and its prediction method of induction heating asphalt concrete, Constr. Build. Mater. 309 (2021) 124920, https://doi.org/10.1016/j.conbuildmat.2021.124920.
[50] C. Sangiorgi, et al., A complete laboratory assessment of crumb rubber porous asphalt, Constr. Build. Mater. 132 (Feb. 2017) 500–507, https://doi.org/10.1016/j.conbuildmat.2016.12.016.
[51] A.E. Alvarez, A.E. Martin, and C. Estakhri, A Review of Mix Design and Evaluation Research for Permeable Friction Course Mixtures, Mar. 2011. doi: 10.1016/j.conbuildmat.2010.09.038.
[52] D. Prieto-Quintana, M.Á. Calzada-Pérez, and P. Lastra-González, Desarrollo de una nueva prueba de control y validación de mezclas porosas, Universidad de Cantabria, 2022. Accessed: Jul. 05, 2024. [Online]. Available: ⟨https://repositorio.unican.es/xmlui/handle/10902/26146⟩.
[53] A.H.A. Alhaddad, Construction of a complex shear modulus master curve for Iraqi asphalt binder using a modified sigmoidal fitting, Int. J. Sci. Eng. Technol. Res. 04 (2015) 0682–0690.
[54] C. Delafuente-Navarro, P. Lastra-González, C. Slebi-Acevedo, I. Indacoechea-Vega, D. Castro-Fresno, Multi-criteria analysis of porous asphalt mixtures with aramid fiber under adverse conditions, Constr. Build. Mater. 429 (2024), https://doi.org/10.1016/j.conbuildmat.2024.136438.
[55] M.E. Barrett, P. Kearfott, J.F. Malina, Stormwater quality benefits of a porous friction course and its effect on pollutant removal by roadside shoulders, Water Environ. Res. 78 (11) (2006) 2177–2185, https://doi.org/10.2175/106143005x82217.
[56] M.L. Afonso, M. Dinis-Almeida, C.S. Fael, Study of the porous asphalt performance with cellulosic fibres, Constr. Build. Mater. 135 (2017) 104–111, https://doi.org/10.1016/j.conbuildmat.2016.12.222.
[57] C. Tingwei, W. Shaopeng, C. Mingyu, L. Juntao, Resistance to permanent deformation and low-temperature cracking of porous asphalt mixture using the tafpack super additive, Mater. Sci. Forum 620 (622) (2009) 347–350, https://doi.org/10.4028/www.scientific.net/MSF.620-622.347.
[58] H. Miera-Dominguez, et al., Design and validation of a new asphalt mixture to reduce road traffic noise pollution in urban areas, Case Stud. Constr. Mater. 20 (Jul. 2024) e03107, https://doi.org/10.1016/j.cscm.2024.e03107.